

A replacement of the Lorentz law for the shape of the spectral lines in the infrared region

A. Carati A.M. Maiocchi*

25 Aprile 2016

Abstract

We propose a new phenomenological law for the shape of the spectral lines in the infrared, which accounts for the exponential decay of the extinction coefficient in the high frequency region, observed in many spectra. We apply this law to the measured infrared spectra of LiF, NaCl and MgF₂, finding a good agreement, over a wide range of frequencies.

Keywords: infrared spectra, multiphonon tails, Lorentz dispersion model

1 Introduction

At a phenomenological level, the experimental data for the complex susceptibility $\hat{\chi}(\omega)$ are fitted by taking for each line a contribution of the form

$$\hat{\chi}(\omega) = \frac{\omega_0 A}{\omega_0^2 - \omega^2 - 2i\gamma\omega}, \quad (1)$$

where ω_0 is the line frequency, γ is related to its width and A to its intensity. This formula was originally obtained by thinking of each line as corresponding to a “physical” microscopic dipole oscillating with frequency ω_0 and with a

*Dipartimento di Matematica, Università degli Studi di Milano, Via Saldini 50, I-20133 Milano, ITALY.

damping characterized by the constant γ . In the literature this is often referred to as the “Lorentz model”. However, some difficulties arise in connection with the imaginary part of the complex susceptibility, which, in the transparency region of dielectrics, dictates the behavior of the extinction coefficient χ .¹ In fact, it is known since the seventies that for dielectrics, in the region of high transparency, the Lorentz formula (1) provides for the extinction coefficient not only a too large value (by orders of magnitude), but also a qualitatively incorrect behavior.

Indeed, relation (1) gives, for the imaginary part,

$$\text{Im } \hat{\chi}(\omega) = \frac{2\gamma\omega_0\omega A}{(\omega^2 - \omega_0^2)^2 + 4\gamma^2\omega^2}, \quad (2)$$

which reduces to the well known Lorentz formula

$$\text{Im } \hat{\chi}(\omega) \simeq \frac{\gamma A/2}{(\omega - \omega_0)^2 + \gamma^2}, \quad (3)$$

for frequencies near the absorption peak, $\omega \simeq \omega_0$. So, formula (2) predicts that the extinction coefficient decreases as ω^{-3} for large ω , whereas, in the transparency region, i.e., for $\omega \neq \omega_0$, the measured values of the extinction coefficient (see [1, 2]) exhibit a decay which is exponential rather than as an inverse power of ω . In the literature (see [3, 4, 5]) one finds ab initio computations which reproduce quite well the experimental findings, and have been successfully adapted, in more recent years, to modeling the absorption coefficients of different materials (see, for instance, [6]). However, the relation between the model parameter and the data are quite involved, and, more important, a simple general reason for the observed behavior is lacking.

In this paper we propose an explanation of the observed exponential decay of the extinction coefficient, as due to the fact that the time auto-correlation of polarization should be an analytic function of time. We also propose a simple phenomenological formula which should be substituted for the Lorentz one, in order to describe the exponential decay of the experimental data. Such a formula involves the asymptotic (in time) behavior of the time auto-correlation of polarization, as described below.

¹As is well known, the susceptibility χ is related to the extinction coefficient χ and the refractive index n by $4\pi \text{Re } \hat{\chi} = n^2 - \chi^2 - 1$ and $4\pi \text{Im } \hat{\chi} = 2n\chi$. So, in the region in which the dielectric is transparent, i.e., where n is approximately constant, the behavior of $\text{Im } \hat{\chi}$ determines the behavior of χ .

In Section 2 the theoretical argument is presented and the corresponding proposed formula is given. In Section 3 a quantitative check of the proposed formula is performed, by fitting the experimental data for three dielectrics (LiF, NaCl, MgF₂) over a very large interval of frequencies in the infrared region. In the last Section 4 some comments are added, in particular concerning the relaxation of the correlations of polarization.

2 The susceptibility according to linear response theory

In modern terms, the Lorentz law (1) can be justified through linear response theory as follows. The susceptibility is nothing but the Fourier transform of the time correlation of polarization: this is a particular case of Green–Kubo formula (see [7]), as explained in detail in [8]. In formulæ, one has²

$$\hat{\chi}(\omega) = -\frac{V}{4\pi k_B T} \int_0^{+\infty} e^{i\omega t} \langle P(0)\dot{P}(t) \rangle dt, \quad (4)$$

where $P(t)$ is the system polarization and the brackets denote a suitable average (for example the canonical one). Now, the classical formula (1) is obtained if one supposes that the correlation occurring in (4) decays exponentially for $t \rightarrow +\infty$ as a damped sinusoid, i.e., that

$$\langle P(0)\dot{P}(t) \rangle \propto -\sin \omega_0 t e^{-\gamma t}.$$

However, if at first sight such an ansatz for the correlation can appear physically sound, one has to recall that the correlation $\langle P(0)\dot{P}(t) \rangle$ is an odd function of time (because it is the derivative of the correlation $\langle P(0)P(t) \rangle$, which has to be even). Thus the correct expression should rather be

$$\langle P(0)\dot{P}(t) \rangle \propto -\sin \omega_0 t e^{-\gamma|t|}, \quad (5)$$

which is **not** an analytic function of time, due to the presence of $|t|$ in the argument of the exponential.

²We are here considering isotropic systems, otherwise a susceptibility tensor should be considered, and the formulæ should be changed accordingly.

This rather abstract remark immediately implies that the imaginary part of susceptibility, and thus the extinction coefficient, cannot decay exponentially if the correlation has the form (5). In fact, from (4) one has

$$\text{Im } \hat{\chi}(\omega) = -\frac{1}{2} \frac{V}{4\pi k_B T} \int_{\mathbb{R}} \sin \omega t \langle P(0) \dot{P}(t) \rangle dt ,$$

which shows that the extinction coefficient decays exponentially if and only if $\langle P(0) \dot{P}(t) \rangle$ is analytic as a function of time.

On the other hand, there is no reason for the appearance of a singularity at $t = 0$ in the expression of the correlation, and it seems instead natural to suppose that $\langle P(0) \dot{P}(t) \rangle$ should be chosen to be an analytic function. So the problem is now reduced to finding a simple analytic function which is odd and decays exponentially. One should however take into account the fact that $\langle P(0) \dot{P}(t) \rangle$ is a correlation, in particular the derivative of the time auto-correlation $\langle P(0) P(t) \rangle$, which is a positive-definite function (in the sense of Bochner, see [9], p. 17). This apparently abstract mathematical requirement in particular implies that the extinction coefficient be positive at all frequencies,³ a very sound physical constraint indeed. We also point out that in our setting, in virtue of the definition (4) of $\hat{\chi}(\omega)$, the Kramers-Kronig relations are automatically satisfied for any correlation which is L^2 integrable in time, in virtue of Titchmarsh's theorem ([10], Theorem 95, see also [8]).⁴

³In fact, since $\langle P(0) P(t) \rangle$ is positive-definite, one has

$$\langle P(0) P(t) \rangle = \int_{\mathbb{R}} d\omega \alpha(\omega) \cos(\omega t) ,$$

with $\alpha(\omega) \geq 0, \forall \omega \in \mathbb{R}$, in virtue of Bochner theorem. Then,

$$\langle P(0) \dot{P}(t) \rangle = - \int_{\mathbb{R}} d\omega \omega \alpha(\omega) \sin(\omega t) ,$$

so that $\text{Im } \hat{\chi}(\omega) = A \omega \alpha(\omega)$ with a suitable constant $A > 0$, and so $\text{Im } \hat{\chi}$ is positive for $\omega \geq 0$.

⁴The Kramers-Kronig relations can be formally shown as follows. Expression (4) shows that $\hat{\chi}(\omega)$ is analytic in the half plane $\text{Im } \omega > 0$. Then, by Cauchy's integral formula, one has

$$\hat{\chi}(\omega) = \frac{1}{2\pi i} \oint_{\Gamma_R} \frac{\hat{\chi}(\omega')}{\omega' - \omega} d\omega' ,$$

where the integration contour Γ_R is chosen as a semicircle of radius R in the upper half plane and its diameter lying on the real axis, while ω is any point in the interior of the contour. Then, by taking the limit for $R \rightarrow \infty$ and supposing that the integral on the semicircle goes to zero,

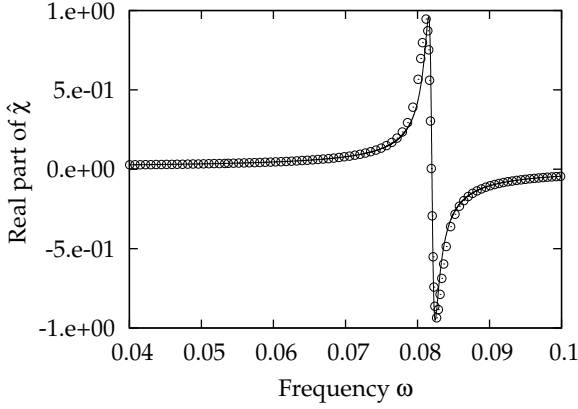


Figure 1: Real part of (8) computed numerically (circles), together with the real part of the Lorentz expression for $\hat{\chi}$ as given in (12), solid line. Here the relevant parameters are $\omega_0 = 0.0818$, $\gamma = 8.01 \cdot 10^{-4}$, $\Omega = 0.082$, $\Gamma = 4.58 \cdot 10^{-4}$.

The simplest choice, in our opinion, is to take

$$\langle P(0)\dot{P}(t) \rangle \propto -\frac{\sin \omega_0 t}{\cosh \gamma t}, \quad (6)$$

which satisfies all the requirements. The Fourier transform of the r.h.s. can be easily expressed in terms of a well-studied function, i.e., the Laplace transform $\mathcal{L}(s)$ of the hyperbolic secant:

$$\mathcal{L}(s) \stackrel{\text{def}}{=} \int_0^{+\infty} \frac{e^{-st}}{\cosh t} dt. \quad (7)$$

Indeed, an elementary computation shows that

$$\int_0^{+\infty} \frac{\sin \omega_0 t}{\cosh \gamma t} e^{i\omega t} dt = \frac{i}{2\gamma} \left[\mathcal{L}\left(\frac{\omega - \omega_0}{i\gamma}\right) - \mathcal{L}\left(\frac{\omega + \omega_0}{i\gamma}\right) \right]. \quad (8)$$

for any ω with $\text{Im } \omega > 0$ one gets

$$\hat{\chi}(\omega) = \frac{1}{2\pi i} \int_{-\infty}^{+\infty} \frac{\hat{\chi}(\omega')}{\omega' - \omega} d\omega'.$$

The Kramers-Kronig relations then follows by passing to the limit for $\text{Im } \omega = 0$ and taking the real and imaginary part of the above relation.

The imaginary part of the r.h.s. above can be expressed in a closed form, since, for any real s ,

$$\operatorname{Re} \mathcal{L}(is) = \operatorname{sech}\left(\frac{\pi s}{2}\right). \quad (9)$$

Thus, the choice (6) for the polarization correlation gives, for the imaginary part of the susceptibility $\hat{\chi}(\omega)$, the relation

$$\operatorname{Im} \hat{\chi}(\omega) \propto \frac{1}{\gamma} \left(\operatorname{sech}\left(\frac{\pi(\omega - \omega_0)}{2\gamma}\right) - \operatorname{sech}\left(\frac{\pi(\omega + \omega_0)}{2\gamma}\right) \right), \quad (10)$$

as can be directly seen also by integrating the l.h.s. of (8) through the residue theorem. It can be easily checked that this expression gives an exponential decay at high frequencies.

There is instead no known closed-form expression for $\operatorname{Im} \mathcal{L}(is)$, i.e., for the real part of $\hat{\chi}(\omega)$. However, some approximating expansions can be found, starting from the following expansions (see [11], p. 191) for the Laplace transform of the hyperbolic secant

$$\mathcal{L}(s) = 2 \sum_{k=0}^{\infty} \frac{(-1)^k}{s + 2k + 1} = \frac{1}{s + \frac{1}{s + \frac{4}{s + \frac{9}{s + \dots}}}}. \quad (11)$$

The continued fraction expansion should be used for large values of s , i.e., far from the peak, where it converges more rapidly than the series expansion. The latter shows, instead, a clear similarity with the expression given by the Lorentz model. In fact, by expanding in series each of the two terms containing $\mathcal{L}(\cdot)$ and summing terms of equal order, the r.h.s. of (8) can be written as

$$2 \sum_{k=0}^{\infty} (-1)^k \frac{\omega_0}{\omega_0^2 + (2k + 1)^2 \gamma^2 - \omega^2 - 2i\gamma(2k + 1)\omega},$$

namely, as a sum of terms of the kind of the form (1). Both the real and the imaginary parts of the above series are, for any fixed value of ω , definitively decreasing alternating series, so that the error introduced by truncating them at order n can be estimated by the first neglected term. This gives an error of

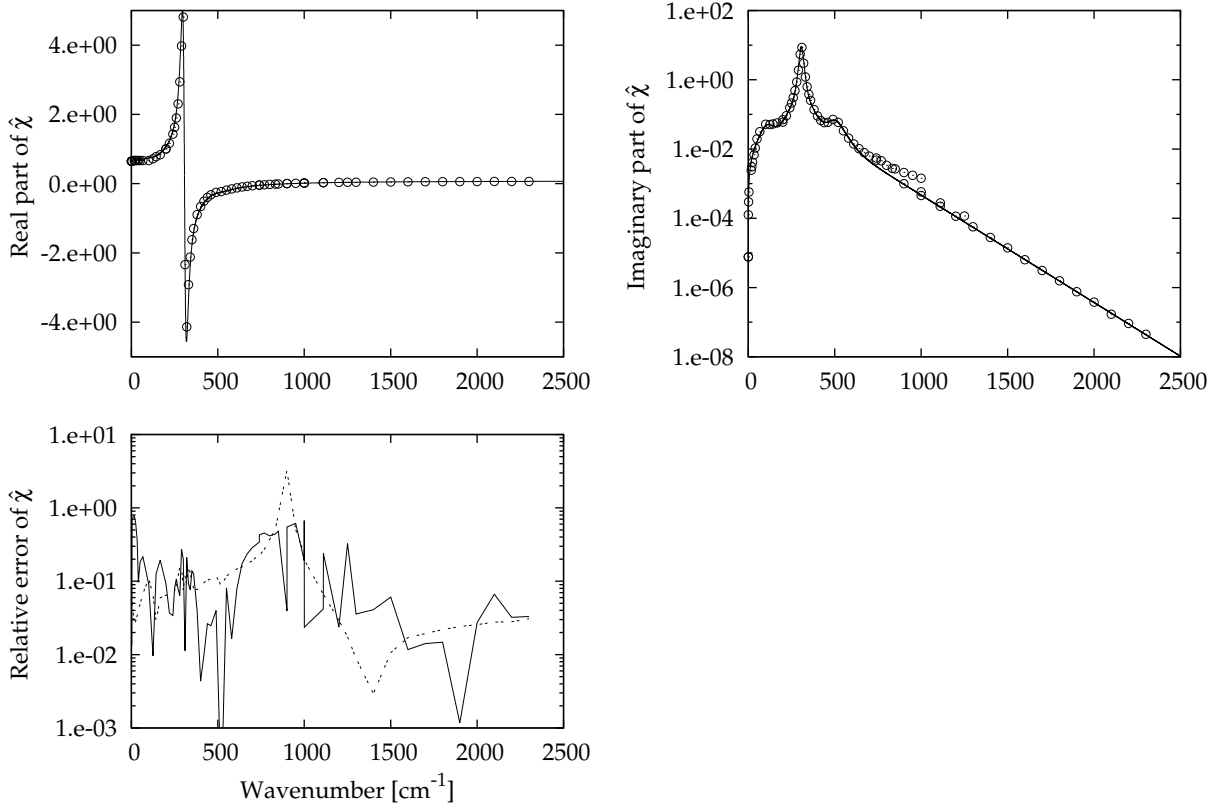


Figure 2: Real (top) and imaginary (centre) parts of susceptibility versus frequency for a LiF crystal. Circles are experimental data taken from [12]. Solid lines represent real and imaginary parts of the fitting function (13), with constants chosen as in Table 1 and $\chi_{\infty} = 7.64 \cdot 10^{-2}$, as given by [13]. The bottom figure displays the relative error of the fit of the real (dashed line) and imaginary (solid line) parts of $\hat{\chi}$.

order $1/n^2$ for the real part and of order $1/n^3$ for the imaginary part. By choosing a sufficiently high order of truncation it is numerically feasible to make the error negligible in comparison with the values of the real part of susceptibility, which are almost everywhere of order 1, but surely not in the tails of the imaginary part, where it becomes exceedingly small. On the other hand, by inspecting Figure 1 it can be checked that a good approximation for the real part

of susceptibility⁵ is given by a single Lorentz model expression

$$\text{Re } \hat{\chi}(\omega) \simeq \Omega A' \frac{\Omega^2 - \omega^2}{(\Omega^2 - \omega^2)^2 + 4\Gamma^2 \omega^2} \quad (12)$$

with suitably chosen constants A' , Ω and Γ . In particular Ω is very close to ω_0 , while Γ turns out to be smaller than γ .

So we propose that formula (10) should be used in place of (2) in fitting the experimental data for the imaginary part of $\hat{\chi}$, which are those actually obtained from the experimental values of n and κ . As an example, we selected three relevant cases of ionic crystals, and showed below that good fits are obtained. Moreover, the parameters entering the fit provide a good approximation also for the real part of susceptibility, as expected.

3 Fit of the susceptibilities of selected crystals

We present here, for three selected elements, the fits of the real and the imaginary parts of susceptibility for three much studied ionic crystals, i.e., LiF, NaCl and MgF₂. Due to the fact that, in general, several lines could be present, we choose to fit the data with the following function

$$\hat{\chi}(\omega) = \hat{\chi}_\infty + \sum_{k=1}^N \frac{iA_k}{2\gamma_k} \left[\mathcal{L}\left(\frac{\omega - \omega_k}{i\gamma_k}\right) - \mathcal{L}\left(\frac{\omega + \omega_k}{i\gamma_k}\right) \right], \quad (13)$$

where i is the imaginary unit, N is the number of terms that should be chosen in order to match the experimental data, $\mathcal{L}(\cdot)$ is the function defined in (11), while $\hat{\chi}_\infty$ is the electronic contribution to susceptibility which, in the infrared region, just reduces to a real constant. The values of the parameters we found are summarized in Table 1, while in Figures 2–4 we plot both the experimental data and the curves found.

For what concerns the experimental data, we recall that only the values of n and κ , and not those of the complex susceptibility $\hat{\chi}$, are usually reported in the literature (see [12] and the references therein). Thus, the complex susceptibility

⁵In all figures the numerical values of $\text{Re } \mathcal{L}(is)$, for real s , are obtained by tabulating such a function. This has been done by truncating at time $T = 40$ the integral (7) which defines \mathcal{L} , and then computing it by a standard fast Fourier transform algorithm with a grid of $N = 2^{20}$ points. We checked that the relative difference with respect to the fast Fourier transform computed with $N = 2^{16}$ is always smaller than $5 \cdot 10^{-3}$ in the region of interest.

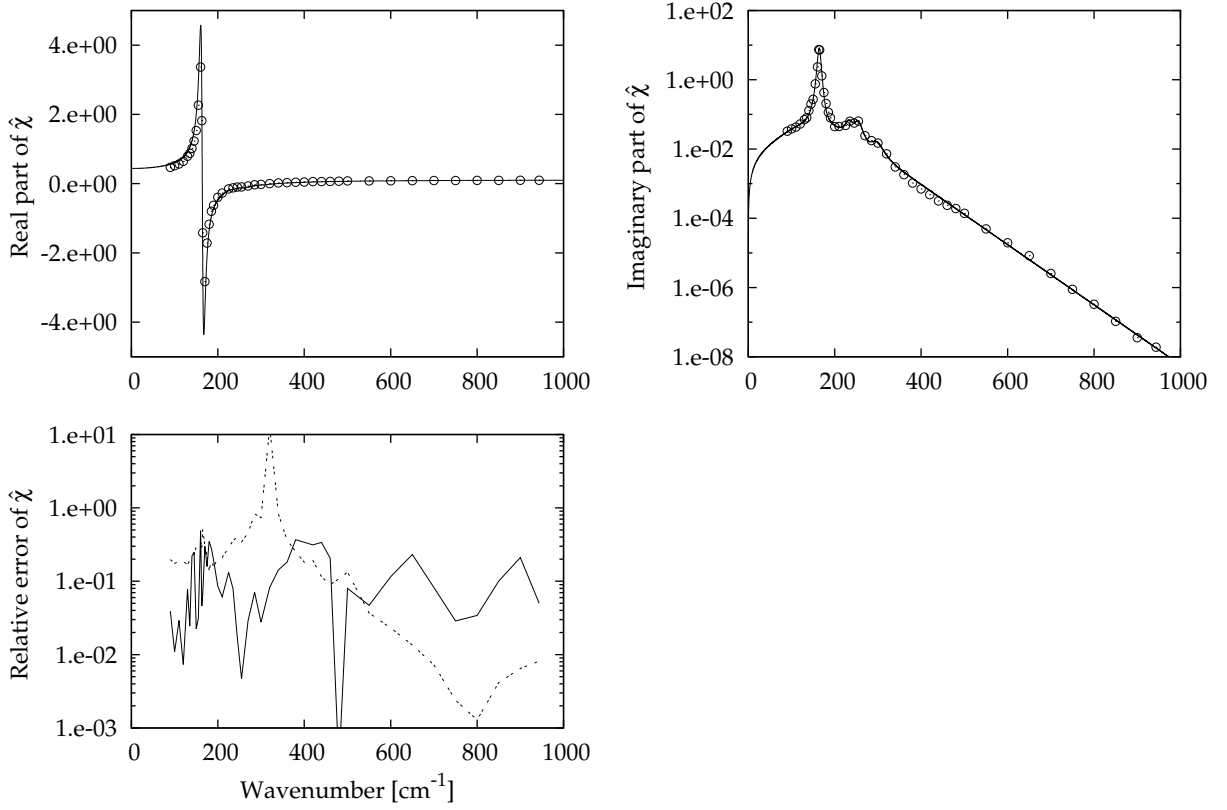


Figure 3: Real (top) and imaginary (centre) parts of susceptibility versus frequency for a NaCl crystal. Circles are experimental data taken from [12]. Solid lines represent real and imaginary parts of the fitting function (13), with constants chosen as in Table 1 and $\hat{\chi}_\infty = 1.08 \cdot 10^{-1}$. The bottom figure displays the relative error of the fit of the real (dashed line) and imaginary (solid line) parts of $\hat{\chi}$.

has to be recovered from the tabulated values of n and χ : this is simple if, for a given frequency, the values of both n and χ are tabulated (see footnote 1). As this is not always the case in the region where n is almost constant, we estimated the refractive index n by linear interpolation when needed.

Two remarks are in order: the first one is that our procedure for determining the parameters, which involves only the imaginary part of susceptibility given by expression (10), was just that of trial and error. In other terms, we find

LiF							
A_k	137	27.8	9.36	3.7	2.29		
ω_k	307	307	307	500	110		
γ_k	12.6	55	220	59	50		
NaCl							
A_k	39.8	6.37	5.57	0.61	0.56	0.193	
ω_k	164	155	161	254	233	296	
γ_k	3.9	79	11	11	11	17	
MgF ₂							
A_k	40.1	38.2	7.32	5.41	3.63	3.06	1.59
ω_k	248	450	407	435	420	485	243
γ_k	6.3	9.4	6.3	27	188	71	39

Table 1: Fitting constants for the function (13), for the three selected substances. All data are expressed in cm^{-1} .

by hands some values of the parameters which, in our opinion, give acceptable fits for the experimental data over a large range of values of $\hat{\chi}$ (nine orders of magnitude). No procedure of error minimization, nor any statistical test, are used to check the quality of the fit. This in particular implies that also the number of terms N in the sum is taken in a sense in an arbitrary way. This point will be discussed below. The data of the real part of susceptibility, which do not enter the fit, are then used for determining the constant $\hat{\chi}_\infty$.

The second remark is that most of the “experimental data” in the region of the “peaks”, are not experimental at all, because in such a region neither the extinction coefficient nor the refractive index can be actually measured. They are actually inferred from other measured quantities (such as the reflectivity) assuming that susceptibility can be described in a fairly good way by the Lorentz model. This is particularly evident in Figure 2, in which two sets of data are present in the region between 800 cm^{-1} and 1000 cm^{-1} . The set of values which presents an exponential decay corresponds to the directly measured values of κ , while the other one contains the values which are inferred from reflectivity measurements.

In view of these two remarks, we expect that the overall accuracy of the fits would be improved if a reprocessing were performed of the experimental data, in the spectral region where the extinction coefficient and the refractive index

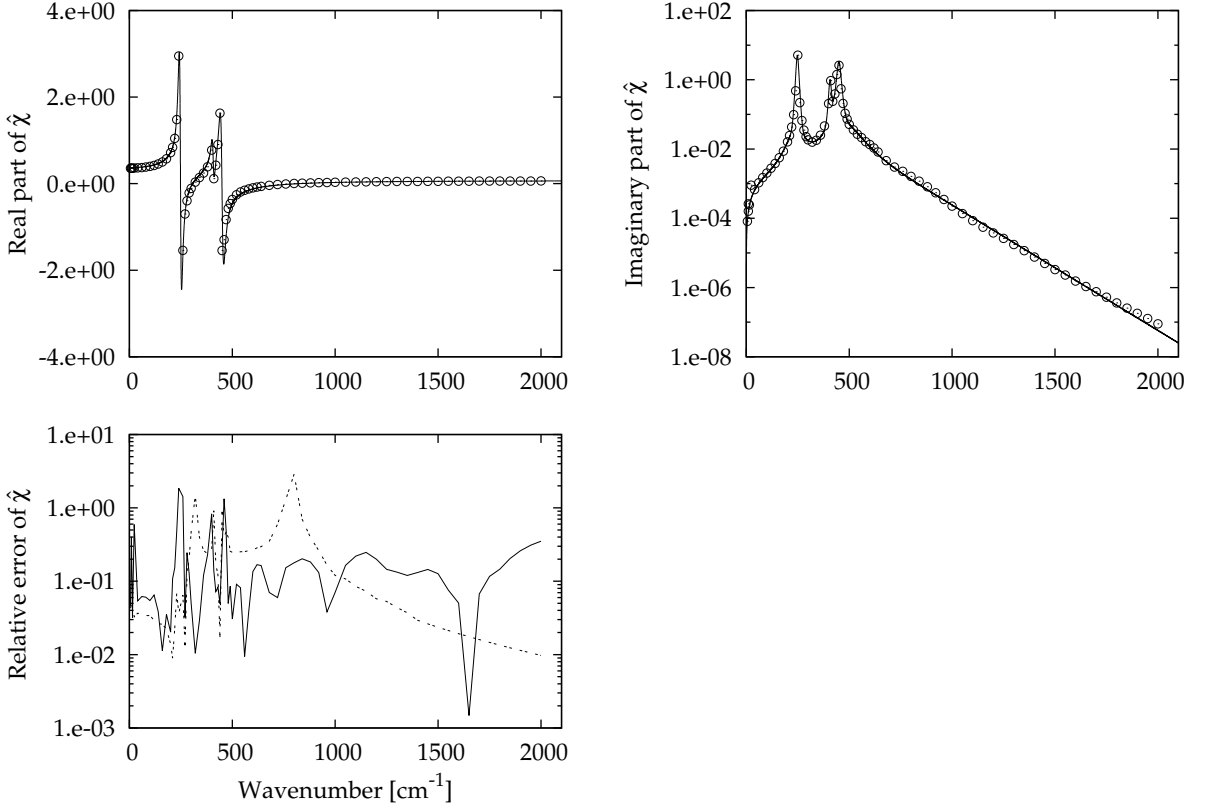


Figure 4: Real (top) and imaginary (centre) parts of susceptibility versus frequency for the ordinary ray in a MgF_2 crystal. Circles are experimental data taken from [12]. Solid lines represent real and imaginary parts of the fitting function (13), with constants chosen as in Table 1 and $\hat{\chi}_\infty = 7.08 \cdot 10^{-2}$. The bottom figure displays the relative error of the fit of the real (dashed line) and imaginary (solid line) parts of $\hat{\chi}$.

are not directly measurable.

We should however take into account the fact that we are dealing here only with a linear response theory, so that the discrepancies can also be due to non-linear effects. These could be particularly relevant close to the peaks, where the polarization is large, and in the regions of very low absorption, where the measurements are performed using laser beams, so that the external field is strong.

4 A final Comment

We discuss here the problem of the number N of terms to be used in the expression (13) for the fit of the imaginary part of susceptibility. Naively, one might expect N to be equal to the number of most “evident” lines, but actually a larger number of terms is needed: in particular (as shown by Table 1) five terms are needed to match the data for LiF, six for NaCl and seven for MgF₂. For example, in order to have a good global fit three different terms have to be associated to the LiF line at 307 cm⁻¹, all with the same frequency, but with three well different damping constants. Something analogous occurs for the NaCl line at about 160 cm⁻¹ and for the MgF₂ line at about 245 cm⁻¹, for both of which several terms of very near frequencies are needed, with however different values of γ .

This can be interpreted by saying that several time-scales are involved in the decay of the relevant correlations, so that the relaxation of the correlations is a much more complicated process than just a simple exponential decay.

This is a well known fact in other fields, for example in glasses (see [14]), or in relaxation spectroscopy (see for example [15]), which involve the behavior of susceptibility at low frequencies (in the micro-waves region), where continuous distributions of relaxation times are actually used. So our result could be read as a hint that, in the infrared region too, the process of the decay of correlations is a complicated one. And indeed, the numerical evidence in some cases seems to support this view. We refer to computations performed by us in the case of a one component model of plasma, see [16], and of a model of LiF crystal, see [17].⁶ In any case, more work is needed to settle this point.

Acknowledgments. We thank prof. L. Galgani for thorough discussions and for his invaluable help in correcting the manuscript.

References

- [1] G. Rupprecht, “Photon-Phonon Interaction in the Near Infrared”, Phys. Rev. Lett. **12**, 580–583 (1964).

⁶In the paper [17] we do not report explicitly the correlation as a function of time. However, an example of such a plot can be found at the following URL: http://fgangemi.unibs.it/LiF_results/avg-corr_na4096-T300_10sim.png

- [2] T.F. Deutsch, “Absorption coefficient of infrared laser window materials”, *J. Phys. Chem. Solids* **34**, 2091–2104 (1973).
- [3] M. Sparks, L.J. Sham, “Theory of Multiphonon Absorption in Insulating Crystals”, *Phys Rev. B* **8**, 3037–3048 (1973).
- [4] M. Sparks, L.J. Sham, “Explicit exponential frequency dependence of multiphonon infrared absorption”, *Phys Rev. B* **9**, 827–829 (1974).
- [5] L.L. Boyer, J.A. Harrington, M. Haas, H.B. Rosenstock, “Multiphonon absorption in ionic crystals”, *Phys Rev. B* **11**, 1665–1680 (1975).
- [6] D.V. Hahn, M.E. Thomas, D.W. Blodgett, “Modeling of the frequency- and temperature-dependent absorption coefficient of long-wave-infrared (2–25 μm) transmitting materials”, *Appl. Opt.* **44**, 6913–6920 (2005).
- [7] R. Kubo, “Statistical-Mechanical Theory of Irreversible Processes. I. General Theory and Simple Applications to Magnetic and Conduction Problems”, *J. Phys. Soc. Jpn.*, **12**, 570–586 (1957).
- [8] A. Carati, L. Galgani, “Classical microscopic theory of dispersion, emission and absorption of light in dielectrics”, *Eur. Phys. J. D* **68**, 307 (2014).
- [9] W. Rudin, *Fourier Analysis on groups*, Wiley-Interscience, New Jersey, 1990.
- [10] E.C. Titchmarsh, *Introduction to the theory of Fourier integrals* (2nd ed.), Oxford University Press, Oxford, 1948.
- [11] S. Khrushchev, *Orthogonal Polynomials and Continued Fractions*, Encyclopedia of Mathematics and Its Application **122**, Cambridge University Press, Cambridge, 2008.
- [12] E. Palik, *Handbook of optical constants of solids* (Academic Press, Amsterdam, 1998).
- [13] A. Kachare, G. Andermann, L.R. Brantley, “Reliability of classical dispersion analysis of LiF and MgO reflectance data”, *J. Phys. Chem. Solids* **33**, 467–475 (1972).
- [14] M.D. Ediger, C.A. Angell, S.R. Nagel, “Supercooled Liquids and Glasses”, *J. Phys. Chem.* **100**, 13200–13212 (1996).

- [15] L. A. Dissado, R. M. Hill, “A Cluster Approach to the Structure of Imperfect Materials and Their Relaxation Spectroscopy”, Proc. Roy. Soc. A **390**, 131–180 (1983).
- [16] A. Carati, F. Benfenati, A. Maiocchi, L. Galgani, “Chaoticity threshold in magnetized plasmas: Numerical results in the weak coupling regime”, Chaos **24**, 013118 (2014).
- [17] F. Gangemi, A. Carati, L. Galgani, R. Gangemi, A. Maiocchi, “Agreement of classical Kubo theory with the infrared dispersion curves $n(\omega)$ of ionic crystals”, EPL **110**, 47003 (2015).